# Chaoticity of the Wet Granular Gas

A. Fingerle,* S. Herminghaus,† and V. Yu. Zaburdaev‡

*Max Planck Institute for Dynamics and Self-Organization*
*Bunsenstr. 10, Germany - 37073 Goettingen*

(Dated: February 1, 2008)

In this work we derive an analytic expression for the Kolmogorov-Sinai entropy of dilute wet granular matter, valid for any spatial dimension. The grains are modelled as hard spheres and the influence of the wetting liquid is described according to the Capillary Model, in which dissipation is due to the hysteretic cohesion force of capillary bridges. The Kolmogorov-Sinai entropy is expanded in a series with respect to density. We find a rapid increase of the leading term when liquid is added. This demonstrates the sensitivity of the granular dynamics to humidity, and shows that the liquid significantly increases the chaoticity of the granular gas.

## I. INTRODUCTION

The field of granular physics has undergone considerable progress in recent times [1, 2]. As part of soft matter physics, granulates have inspired the development of non-equilibrium statistical mechanics [3, 4]. Its potential to the foundation of physics can hardly be over estimated, since granular gases provide a road away from the well-developed Boltzmann-Enskog theory of conservative gases towards dissipative systems far from thermal equilibrium. In connection with geophysics, some aspects of landslides may be understood in terms of a solid-liquid phase transitions of wet granular matter [5, 6, 7], and wet granular gases are of technological relevance in granulators, pelletizers, and other instances in process engineering.

Wet granular gases are systems consisting of mesoscopic particles and a liquid phase wetting the particles. Despite their importance, the theory of wet granular matter is still nascent. There is a growing number of experimental [8] and numerical work [9] on this subject, but the hysteretic nature of the liquid bridge interaction was not taken into account in the modelling. We stress that the attraction force mediated by capillary bridges is not a function of distance but depends on the collision history. The theory of wet granular matter advanced with recent simulation and models describing the free cooling state [10, 11]. To the best of our knowledge, the hysteretic dissipative dynamics of wet granular matter was treated analytically first in [12]. In this article we elaborate on this approach which treats the wet granulate as a complex dynamical system and uses powerful tools available in this area. Such is the Lyapunov spectrum,

$$\lambda_j = \lim_{t \to \infty} \frac{1}{t} \ln \frac{\delta\Gamma_j(t)}{\delta\Gamma_j(0)} \ . \tag{1}$$

It gives the rate of exponential divergence or convergence of two equal copies of the system in phase space, $\delta\Gamma_j(t) = \Gamma_j^{(1)}(t) - \Gamma_j^{(2)}(t)$, with perturbed initial conditions $\delta\Gamma_j(0)$. A positive Lyapunov exponent indicates chaotic behavior, i.e. sensitive dependence on the initial conditions [13]. Since we are dealing with a closed system the sum of all positive Lyapunov exponents equals the Kolmogorov-Sinai entropy (KSE) [14, 15].

The KSE is an indispensable tool in the modern description of dynamical systems. Firstly, from it we learn about the degree of chaoticity because its inverse is the time scale of predictability. Secondly, this dynamical entropy is a well-defined quantity for both equilibrium and non-equilibrium systems. Thirdly, when tiny deviations of initial conditions that were not observable in the beginning are enlarged by the evolution, this can be interpreted as the production of information about the initial conditions. Finally, the KSE is known to be related to macroscopic properties such as transport coefficients [16, 17, 18, 19, 20, 21, 22].

Our objective is to compute the KSE for the wet granular gas. Pioneering work has been done by H. van Beijeren, J. R. Dorfman *et al.* [23, 24] in the analytic treatment of sums of Lyapunov exponents for the gas of hard elastic spheres. We develop a generalization of the method suggested in [23].

This article is organized as follows. In section II we describe in detail the hysteretic interaction of wet granulates. This Capillary Model allows the sticking of particles by attractive forces in contrast to the "Standard Model" for dry granulates which assumes that a certain fraction of energy is lost instantaneously by inelastic collisions. In section III we use the terminology developed in section II to relate the behavior of the two-particle system to the full $N$-particle system. Thereby we are lead to determine the probability distribution for colliding pairs of particles in section IV. In section V we derive the formula that expresses the expansion of velocity space as a function of the two-particle initial conditions for arbitrary spatial dimension. In section VI the results of the sections III-V are combined to accomplish the computa-
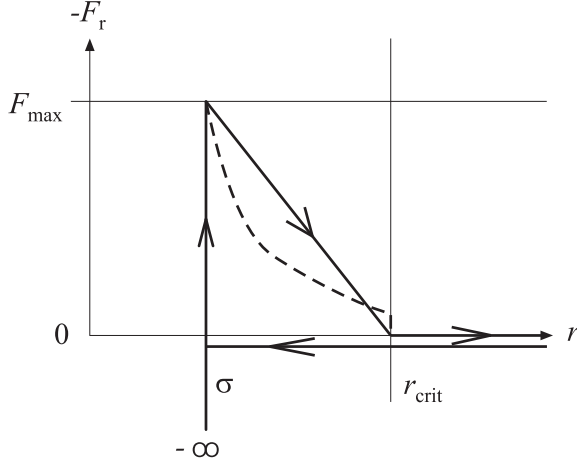
FIG. 1: Radial forces between a pair of wetted spheres. Solid line: The radial force of the Extended Capillary Model is plotted versus the center distance $r$. There is no interaction between the particles as they approach. After the collision applies $\vec{F}(r) = -F_{\max} \frac{r_{\mathrm{crit}}-r}{r_{\mathrm{crit}}-\sigma} \frac{\vec{r}}{r}$ for $r \in (\sigma, r_{\mathrm{crit}})$, otherwise there is no force. Dashed line: Experiments yield a decreasing force law [25, 26] with a discontinuity at the rupture. Therefore the even simpler Minimal Capillary Model which assumes a constant force that drops to zero at the critical separation is a good alternative approximation. The hysteretic interaction is the relevant property which is described by both the Minimal and the Extended Capillary Model.

tion of the KSE.

## II. THE CAPILLARY MODEL

There is an experimentally well confirmed Capillary Model for the dynamics of wet granulates, that will be applied here [7]. The system consists of hard spherical grains with equal diameter $\sigma$ and equal mass $m$. These are covered by a liquid film, so that every time two particles touch, a liquid bridge is formed. The Capillary Model assumes that bridges are formed instantaneously. As we focus on the dilute gas, we may restrict our considerations to pair interactions.

Experiments and computations [25, 26] yield a capillary force law that is excellently described by

$$F = \frac{\pi \gamma \sigma \cos \theta_{\mathrm{w}}}{1 + 0.74\, \mathsf{s} + 1.25\, \mathsf{s}^2} \tag{2}$$

with the wetting angle $\theta_{\mathrm{w}}$, the surface tension $\gamma$, and $\mathsf{s} = s\sqrt{\sigma/V_{\mathrm{bridge}}}$ being the surface separation $s$ expressed in the natural length unit $\sqrt{V_{\mathrm{bridge}}/\sigma}$ of the liquid bridge volume $V_{\mathrm{bridge}}$. The Capillary Model assumes that the bridge pinches off at a critical surface separation $s = s_{\mathrm{crit}}$ (i.e. at a distance $r_{\mathrm{crit}} = \sigma + s_{\mathrm{crit}}$ of the centers). To leading order, the rupture distance $s_{\mathrm{crit}}$ equals the cubic root of the bridge volume $V_{\mathrm{bridge}}$. The energy that was stored

in the stretched liquid bridge before the rupture is dissipated into the liquid and lost for the granular motion. We emphasize that this is the only dissipative mechanism in the Capillary Model (cf. the review article [5], especially Fig. 7 therein, for the capillary regime in which the Capillary Model applies.) In the moment of the rupture, the system is non-Hamiltonian because the atomic degrees of freedom of the liquid to which energy flows are masked out in the description of the granular dynamics. Of course the forces acting on the grains are finite at the rupture, so that the trajectories (as functions of time) are continuous in the granular phase space and differentiable with respect to the initial state before the rupture.

By a collision we denote the moment when two particles in the entire $N$-particle system touch each other. Since we are interested in statistical statements and a point in time is of measure zero, we can assume without loss of generality that there is a unique sequence of collisions. For a certain pair of colliding particles, we refer to the "collision cycle" as the time interval $[t_{\mathrm{i}}, t_{\mathrm{f}}]$ that comprises the collision of these two particles. The collision cycle starts at $t_{\mathrm{i}}$ when the last particle of the two breaks free from its former collision partner and ends at $t_{\mathrm{f}}$ in the moment when the liquid bridge between them ruptures.

During its collision cycle the radial motion of the two-particle system traverses a hysteresis loop. This is shown in Fig. 1 for the force (2) (dashed line) and for a simpler force law (solid line). The solid line in Fig. 1 falls off linearly with the surface separation $s$. This is the Extended Capillary Model in contrast to the Minimal Capillary Model of [7] which assumes a constant force. The corresponding hysteretic "potential" of the Extended Capillary Model is

$$\frac{\phi(r)}{E_{\mathrm{loss}}} = \begin{cases} -1, & \sigma < r \quad \text{before first collision}, \\ -\left(\frac{r_{\mathrm{crit}}-r}{r_{\mathrm{crit}}-\sigma}\right)^2, & \sigma < r \leq r_{\mathrm{crit}} \quad \text{after collision}, \\ 0, & r_{\mathrm{crit}} \leq r \quad \text{after collision}, \\ \infty, & r < \sigma. \end{cases} \tag{3}$$

In both, the Minimal and the Extended Capillary Model, the hysteretic loss of energy, i.e. the area $E_{\mathrm{loss}} = -\int_{\sigma}^{\sigma+s_{\mathrm{crit}}} F_{\mathrm{r}}\, \mathrm{d}r$ in Fig. 1, is a characteristic system property. When the energy in the center of mass system is below $E_{\mathrm{loss}}$, colliding particles will form a stable bound state with periodic collisions. With faster relative motion the liquid bridge exists for a finite time until the particles scatter off each other. We define a corresponding relative velocity $v_{\mathrm{loss}}$ by $E_{\mathrm{loss}} = m v_{\mathrm{loss}}^2/4$ (with the additional factor $1/2$ because $m/2$ is the reduced mass). From this point on we distinguish between scattering events and collisions leading to bound states. For the scattering, the restitution coefficient $\epsilon = E_{\mathrm{f}}/E_{\mathrm{i}}$ of the Capillary Model is an increasing function of the initial energy or velocity:

$$\epsilon(E_{\mathrm{i}}) = \sqrt{1 - \frac{E_{\mathrm{loss}}}{E_{\mathrm{i}}}} \quad \text{or} \quad \epsilon(v_{\mathrm{i}}) = \sqrt{1 - \frac{v_{\mathrm{loss}}^2}{v_{\mathrm{i}}^2}}\, . \tag{4}$$

The binding threshold $E_{\mathrm{loss}}$ of the Capillary Model contrasts sharply with the widespread models for dry gran-
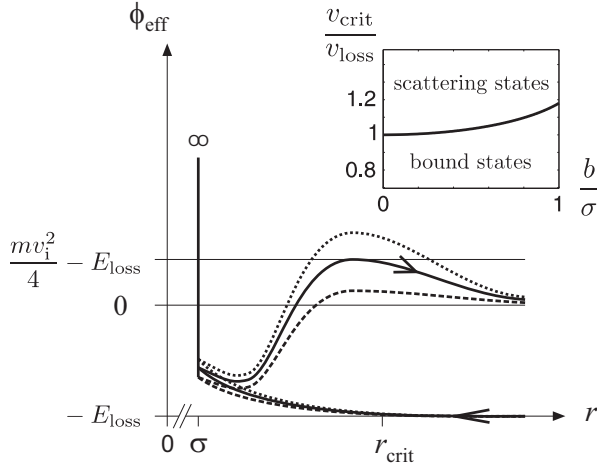
FIG. 2: The effective potential for $v_i > v_{loss}$ and three different impact parameters. For the solid line in the middle $b$ and $v_i$ are critical. For the higher $b$ (fine dotted line) the particles are bound, for a lower $b$ (roughly dotted line) they scatter. The inset shows the complete space of collision parameters. The critical velocity $v_{crit}$ (plotted in units of $v_{loss}$ for $r_{crit} = 2\sigma$) as a function of the scaled impact parameter $b/\sigma$ divides the plane in bound and scattering states.

ules that assume either a constant or with increasing velocity decreasing coefficient of restitution for the collision of viscoelastic particles [2], [36].

Let us denote by $v_{crit}$ the critical modulus of the relative velocity $\vec{v}_i \equiv \vec{v}_1 - \vec{v}_2$, that determines wether the incoming particles will form a bound state or scatter. For head-on collisions (impact parameter $b = 0$) $v_{crit} = v_{loss}$, otherwise $v_{crit} > v_{loss}$ since there is additional energy in the rotary motion. The next step is to determine $v_{crit}$ as a function of $b$.

### Determination of the Critical Velocity

The bridge interaction is a central force problem. If $v_i$ is lower than $v_{loss}$, the effective potential

$$\phi_{eff}(r) = \frac{mb^2 v_i^2}{4r^2} + \phi(r) \qquad (5)$$

(of the liquid bridge potential given by (3)) does not reach a maximum in $r$ after the collision and leads to a bound state. For most $v_i > v_{loss}$ the particles scatter, but there are some bound cases with high angular momenta, corresponding to high impact parameters. Figure 2 shows three effective potentials for a given initial velocity $v_i$ and different impact parameters $b$. In the case drawn with solid lines, $b$ and $v_i$ fulfill the critical relation $v_i = v_{crit}(b)$. For the higher $b$ (fine dotted line in Fig. 2) we have $v_i < v_{crit}(b)$ so that a bound system is formed. Hence the criterion is that $\phi_{eff}(r)$ touches the asymptotic energy $E_{loss} - m v_i^2/4$ in a single point. For the Extended Capillary Model it is possible to calculate these intersections explicitly. These are the roots of $\left(E_{loss} - m v_i^2/4 + \phi_{eff}\right) r^2$, which is a fourth order polynomial in $r$ with one trivial root at $r = 0$ and another unphysical root for $r < \sigma$. So there are two real roots for the bound state which turn into a complex conjugated pair of roots for the scattering state. (Since the derivative of $\phi_{eff}$ is continuous and negative at $r = r_{crit}$, the turning point $r_{max}$ of a bound state follows correctly from this analytic consideration to be $r_{max} < r_{crit}$ without the need to take the non-analytic point $r = r_{crit}$ of $\phi_{eff}$ into account.) The easiest way is to compute the discriminant of the fourth order polynomial $\left(E_{loss} - m v_i^2/4 + \phi_{eff}\right) r^2$, which is equal to

$$
\begin{aligned}
& 16v^4 \; \underline{b^4} \\
+\; & \left(8v^6 - 4v^4 \left(5\gamma + 9\right) + v^2 \left(27 + 18\gamma - \gamma^2\right)\right) \; \underline{b^2} \\
-\; & v^6 + v^8 + 3v^6\gamma + 3v^4 \left(\gamma - 1\right)\gamma + v^2 \left(\gamma - 3\right)\gamma^2 - \gamma^3 \,,
\end{aligned}
$$

with $\gamma = \sigma \frac{2r_{crit} - \sigma}{(r_{crit} - \sigma)^2}$. The discriminant vanishes as the two physical roots coincide. Since the impact parameter $b$ enters the problem only trough the angular momentum term in (5), the discriminant is a quadratic function of $b^2$. Therefore it is elementary to give $b_{crit}(v_i)$ as the inverse function of $v_{crit}(b)$ explicitly:

$$\frac{b_{crit}(v_i)}{\sigma} = \frac{\sqrt{-8 - 20\delta^2 + \delta^4 + 16w^2 + 20\delta^2 w^2 - 8w^4 - \delta \left(8 + \delta^2 - 8w^2\right)^{3/2}}}{4\sqrt{2} w(\delta - 1)} \,, \qquad (6)$$

with $\delta = \frac{r_{crit}}{r_{crit} - \sigma}$ and $w = \frac{v_i}{v_{loss}}$. This function is plotted as inset in Fig. 2. Much more concise is the corresponding function for the Minimal Capillary Model:

$$v_{crit}(b) = \frac{v_{loss}}{\sqrt{1 - \frac{b^2}{r_{crit}^2}}} \,. \qquad (7)$$
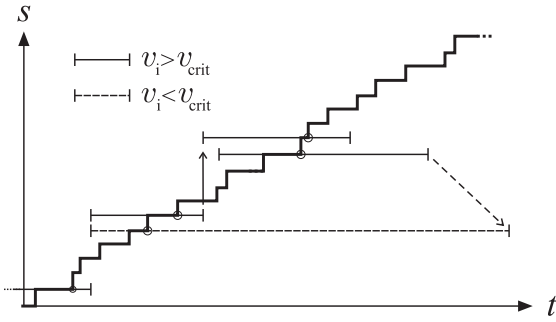
FIG. 3: The collision sequence $s(t)$ and the collision cycles: the step function $s(t)$ is the total number of collisions in the entire $N$-particle system until time $t$. The horizontal solid and dashed bars symbolize the collision cycles for scattering and bound pairs respectively. For the derivation is important that overlapping cycles affect different pairs of particles. The dashed arrow indicates a third particle that hits and breaks up a bound two-particle state.

In the following sections including the main results (41)-(44) of this article, we shall be completely general without the need to specify for the Minimal or Extended Capillary Model.

## III. HOW TO RELATE THE TWO-PARTICLE SYSTEM TO THE $N$-PARTICLE SYSTEM

In the previous section we have shown how on the level of two-particle interactions the most important property of the real wet granular gas, namely the hysteretic binding and breaking of liquid bridges, can be modelled. Further, we have seen that the bond energy of the liquid bridge gives rise to the sticking of particles. In this section we treat the many-particle system.

Let $\nu$ denote the mean collision frequency per particle. If the modulus of the initial relative velocity $v_i$ is lower than $v_{crit}$, so that particles stick together, the collision cycle is not terminated until a third particle bumps into the bound two-particle system. We assume that the out-state of such a three-particle event contains free particles, because the formation of higher mass clusters is rare in the gas-like state (cf. Fig. 10). The pair interactions taking place in the $N$-particle system may be envisaged as shown in Fig. 3. The number of collisions up to time $t$ is denoted by $s(t)$. Since $s(t)$ is strictly monotonic its inverse $t(s)$ exists. The collision rate of the system, $s/t(s)$, tends for $s \to \infty$ to $N\nu/2$ (each collision involves two particles). To have the steps visible Fig. 3 has been drawn for low $N$. The horizontal bars represent the concept of collision cycles introduced in the last section. There are two particles which are going to collide. As the beginning of the collision cycle we take the time when the last of these two particles has ruptured its liquid bridge connection to some previous collision partner. The collision cycle will end when these two particles rupture the liquid

bridge between them. Thus a solid arrow in Fig. 3 shows that one of the particles which just finished its collision cycle immediately begins another one. The dashed arrow indicates that a third particle (that came out of another collision cycle) ends a bound two-particle state.

With this picture in mind the computation of the KSE can be tackled. As stated by Pesin's theorem the KSE equals the sum of all positive Lyapunov exponents, because the system is closed and sufficient chaotic [14]. Lyapunov exponents describe the rate at which a certain direction in phase space grows or shrinks for large times. There is a orthogonal set of Lyapunov vectors $\xi_j$ describing the direction while the associated Lyapunov exponent $\lambda_j$ describes the exponential rate

$$\xi_j(t) \simeq \xi_j(0) \, e^{\lambda_j \, t} \tag{8}$$

for long times $t$. According to the sign of $\lambda_j$ one speaks of stable or unstable directions. The deviations in the initial conditions are infinitesimal small, i.e. the Lyapunov exponents characterize the tangent space map associated with a certain trajectory. In an ergodic system the Lyapunov spectrum $\{\lambda_j\}$ is independent of the trajectory according to Oseledec's theorem [27]. There is no doubt about the ergodicity of the gas of $N \gg 1$ hard spheres [28].

Since in a dilute system the free flight time and the mean free path are large compared to the interaction time and the range $r_{crit}$ of the interaction, perturbations of velocities are amplified as compared to spatial deviations [23]. This is not to be understood as a neglect of the spatial Lyapunov exponents. The Capillary Model is symplectic [11] so that for each positive exponent $\lambda_j$ there is a negative exponent $\lambda_k = -\lambda_j$ and the fact that the spatial deviations remain small means that the spatial directions mainly contain negative Lyapunov exponents, while the positive ones are assigned to velocities. So the conjecture is that the velocity space coincides (approximately) with the unstable manifold of the system. Based on this conjecture the KSE, $h_{KS}$, is given by the logarithmic volume growth rate in velocity space:

$$h_{KS} = \lim_{s \to \infty} \frac{1}{t(s)} \, \ln \left| \det \prod_{i=1}^{s} M_i \right| . \tag{9}$$

The deviation matrix $M_i$ of the $i$'s collision cycle is restricted to velocity space, so that it describes the evolution of velocity perturbations. There are three crucial points here: (i) This limit exists by virtue of Oseledec's multiplicative ergodic theorem [27]. (ii) We have an unique collision sequence. (iii) Although there are pair interactions occurring with time overlaps, there is no ordering problem when writing down the total deviations as a product of collision cycles, because the co-existing liquid bridge interactions affect always disjoint pairs (by the assumption that there are two-particle clusters only) and deviation matrices of disjoint pairs commute. Therefore the matrices $M_i$ can describe the full collision cycle of a single pair of particles, ignoring all

other interactions taking place simultaneously in the $N$-particle system. Our approach differs from [23], because the Capillary Model has a hysteretic interaction with finite interaction time. The dry limit follows by turning off the interaction, $E_{\text{loss}} \to 0$, as a special case.

The expression (9) can be simplified dramatically:

$$
\begin{aligned}
\frac{h_{\text{KS}}}{N} &= \frac{1}{N} \lim_{s \to \infty} \frac{1}{t(s)} \ln \left| \det \prod_{i=1}^{s} M_i \right| \\
&= \frac{1}{N} \lim_{s \to \infty} \frac{1}{t(s)} \sum_{i=1}^{s} \ln |\det M_i| \\
&= \frac{1}{N} \lim_{s \to \infty} \frac{s}{t(s)} \frac{\sum_{i=1}^{s} \ln |\det M_i|}{s} \\
&= \frac{\nu}{2} \langle \ln |\det M| \rangle \; .
\end{aligned}
\tag{10}
$$

Herein the brackets $< \ldots >$ denote averaging over the two-particle phase space only.

Since we expect the Lyapunov exponents to be of the order of the collision frequency $\nu$, they are (according to the limit in (9)) only well-defined if we let the system evolve for a time

$$
t_{\text{Lyapunov}} \gg \frac{1}{\nu} = t_{\text{coll}} \; .
$$

In the subsequent discussion we will point out that this can be fulfilled even if there was no external driving mechanism to keep the dissipative system in a stationary state. Clearly, without a thermostat the system cools, $\dot{T} < 0$, [10, 11]. The collision frequency $\nu$ is of the order $|\dot{T}|/E_{\text{loss}}$. On the other hand, cooling will be irrelevant on time scales below $t_{\text{cool}} = T/|\dot{T}|$ . So the hierarchy

$$
t_{\text{coll}} \ll t_{\text{Lyapunov}} \ll t_{\text{cool}}
$$

of time scales can be fulfilled if

$$
E_{\text{loss}} \ll T \; .
\tag{11}
$$

This implies that for weak liquid bridges as compared to the thermal energy we may speak of a Lyapunov spectrum independently from the question of the thermostat. No additional limitation is set, since the condition (11) is already required to be consistent with the gas state (displaying mainly single particles instead of clusters) which is studied in this work.

Two tasks remain. The determination of the probability distribution for the formula (10) is done in the next section. To make use of momentum conservation the subspace is spanned by the center of mass position $\vec{R} \equiv \frac{\vec{r}_1 + \vec{r}_2}{2}$ and velocity $\vec{V} \equiv \frac{\vec{v}_1 + \vec{v}_2}{2}$ of the two-particle system, as well as the distance $\vec{r} \equiv \vec{r}_1 - \vec{r}_2$ between the centers of the spheres and their relative velocity $\vec{v} \equiv \vec{v}_1 - \vec{v}_2$. The last step is to compute for any spatial dimension $D$ the matrix $M$ appearing in (10), which maps for a specific point in the $4D$-dimensional phase space $(\vec{R}, \vec{r}, \vec{V}, \vec{v})$ the

initial velocity deviations

$$
\begin{pmatrix} \delta \vec{V}_{\text{i}} \\ \delta \vec{v}_{\text{i}} \end{pmatrix}
\tag{12}
$$

from the beginning of the collision cycle to the final deviations

$$
\begin{pmatrix} \delta \vec{V}_{\text{f}} \\ \delta \vec{v}_{\text{f}} \end{pmatrix} = M \begin{pmatrix} \delta \vec{V}_{\text{i}} \\ \delta \vec{v}_{\text{i}} \end{pmatrix}
\tag{13}
$$

at the end of the collision cycle. This is done in section V.

Before we derive the joint probability density a comment on the velocity distribution itself is in order. It is well-known that for dissipative gases the velocity distribution can deviate from the Maxwell-Boltzmann velocity distribution [29] depending on the state and driving mechanism. For explicit results we shall use the Maxwell-Boltzmann velocity distribution,

$$
\begin{aligned}
P(v_1, v_2) \, \mathrm{d}^D v_1 \, \mathrm{d}^D v_2 &= \left( \frac{\alpha}{\pi} \right)^D \mathrm{e}^{-\alpha(v_1^2 + v_2^2)} \, \mathrm{d}^D v_1 \, \mathrm{d}^D v_2 \\
&= \left( \frac{\alpha}{\pi} \right)^D \mathrm{e}^{-\alpha(2V_{\text{i}}^2 + \frac{1}{2} v_{\text{i}}^2)} \, \mathrm{d}^D V_{\text{i}} \, \mathrm{d}^D v_{\text{i}} \\
&= P(V_{\text{i}}, v_{\text{i}}) \, \mathrm{d}^D V_{\text{i}} \, \mathrm{d}^D v_{\text{i}}
\end{aligned}
\tag{14}
$$

with $\alpha = \frac{m}{2T}$. The result for the KSE will also be given in a form that is readily evaluated for any velocity distribution. For the distribution (14) the modulus $v_{\text{i}}$ of the initial relative velocity is distributed according to

$$
P(v_{\text{i}}) \, \mathrm{d}v_{\text{i}} = \frac{2 \left( \frac{\alpha}{2} \right)^{\frac{D}{2}}}{\Gamma \left( \frac{D}{2} \right)} v_{\text{i}}^{D-1} \, \mathrm{e}^{-\frac{\alpha}{2} v_{\text{i}}^2} \, \mathrm{d}v_{\text{i}} \; .
\tag{15}
$$

## IV. THE ENSEMBLE AVERAGE

We determine the probability distribution for two particles under the condition that they will collide in the future. Therefore we depict the initial configuration of an arbitrary pair of particles in relative coordinates $\vec{r}_{\text{i}} = \vec{r}_1 - \vec{r}_2$ as follows (Fig. 4): we rotate our coordinate frame such that the horizontal axis is per definition

$$
\vec{e}_x \equiv \frac{\vec{v}_{\text{i}}}{v_{\text{i}}} \; ,
\tag{16}
$$

with the initial relative velocity $\vec{v}_{\text{i}} = \vec{v}_1 - \vec{v}_2$. This means that particle 2 rests in the origin while particle 1 moves horizontally to the right. Clearly, the particles will collide if and only if

$(i)$    the impact parameter is low enough,

$$
b = \sqrt{r_{\text{i}}^2 - \left( \vec{r}_{\text{i}}, \frac{\vec{v}_{\text{i}}}{v_{\text{i}}} \right)} \leq \sigma,
$$

$(ii)$    and particle 1 is to the left of particle 2,
$(\vec{r}_{\text{i}}, \vec{v}_{\text{i}}) < 0.$
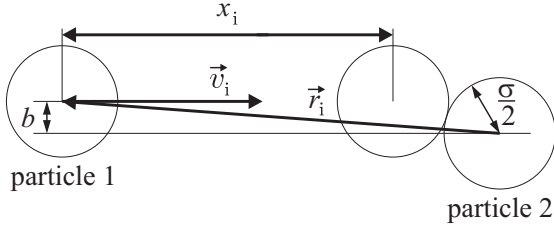
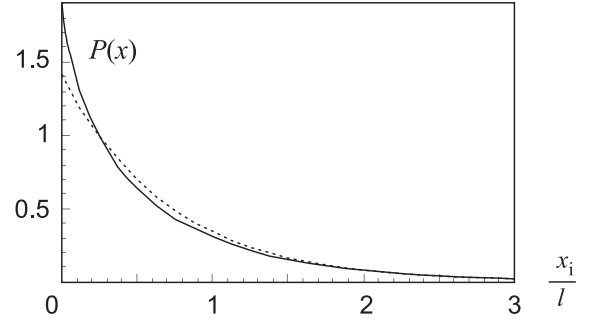FIG. 4: The relative coordinate system with respect to particle 2.



FIG. 5: The distribution of $x_i$ after averaging out the velocities. The dashed curve is an exponential distribution with the same mean. Clearly $P(x_i)$ deviates from an exponential at distances $x_i$ below the mean free path $l$.

For any pair of velocities $\vec{v}_1, \vec{v}_2$, there are initial relative spatial positions that lead to a collision. So we have to integrate over the entire velocity space $\mathbb{R}^D \times \mathbb{R}^D$,

$$\left(\frac{\alpha}{\pi}\right)^D \int_{\mathbb{R}^D} \mathrm{d}^D v_1 \int_{\mathbb{R}^D} \mathrm{d}^D v_2 \; \mathrm{e}^{-\alpha\left(v_1^2+v_2^2\right)} \; . \quad (17)$$

We take condition $(i)$ into account by integrating the impact parameter over the interval $[0, \sigma]$. From the conventional assumption of molecular chaos (i.e. the positions and velocities of two particles are uncorrelated) follows that the impact is uniformly distributed within the cross section,

$$P(b) \, \mathrm{d}b = (D-1)\frac{b^{D-2}\,\mathrm{d}b}{\sigma^{D-1}}, \; 0 < b < \sigma \; . \quad (18)$$

Further, we need to know the horizontal distance $x_i > 0$ to the collision point. Together with the impact parameter $b$ this determines the relative spatial position completely in the plane of incidence, since according to $(ii)$, $\vec{r} = b\,\vec{e}_y - (x_i + \sqrt{\sigma^2 - b^2})\,\vec{e}_x$ always points to the left.

The probability distribution of $x_i$ follows from the distance covered by the particles in the laboratory frame. Denoting by $x_1$ and $x_2$ the length that particle 1 and 2, respectively, have travelled in the laboratory frame since the beginning of the collision cycle, we have the equal time condition

$$\frac{x_1}{v_1} = t_{\mathrm{free}} = \frac{x_2}{v_2} \; , \quad (19)$$

where $t_{\mathrm{free}}$ stands for the time of free flight that both particles have in common. From this follows for the initial separation of particles

$$x_i = v_i \, t_{\mathrm{free}} = \frac{v_i}{v_1} x_1 \; . \quad (20)$$

The probability density of the travelled distances $x_1$ and $x_2$ are known in a gas to be

$$\mathrm{e}^{-x_j/l} \, \frac{\mathrm{d}x_j}{l} \; , \quad j = 1, 2. \quad (21)$$

The length scale $l$ is the mean free path in the laboratory frame. Hence, under the assumption of molecular chaos

the probability density of the initial separation $x_i$ is

$$\begin{aligned}
P(x_i|v_1, v_2) &= C \int_0^\infty \frac{\mathrm{d}x_1}{l} \int_0^\infty \frac{\mathrm{d}x_2}{l} \; \mathrm{e}^{-(x_1+x_2)/l} \\
&\quad \times \delta\left(x_i - x_1\frac{v_i}{v_1}\right) \delta\left(\frac{x_1}{v_1} - \frac{x_2}{v_2}\right) \\
&= C' \, \mathrm{e}^{-\frac{x_i}{l}\frac{v_1+v_2}{v_i}}
\end{aligned}$$

up to a normalization factor. Obviously this yields the integration

$$\frac{v_1 + v_2}{v_i} \int_0^\infty \frac{\mathrm{d}x_i}{l} \; \mathrm{e}^{-\frac{x_i}{l}\frac{v_1+v_2}{v_i}} \quad (22)$$

as part of the ensemble average. Putting (17), (18) and (22) together we can compute arbitrary expectation values:

$$\begin{aligned}
\langle \ldots \rangle &= (D-1)\left(\frac{\alpha}{\pi}\right)^D \int_{\mathbb{R}^D} \mathrm{d}^D v_1 \int_{\mathbb{R}^D} \mathrm{d}^D v_2 \, \frac{v_1+v_2}{v_i} \\
&\quad \times \int_0^\sigma \frac{\mathrm{d}b\,b^{D-2}}{\sigma^{D-1}} \int_0^\infty \frac{\mathrm{d}x_i}{l} \\
&\quad \times \mathrm{e}^{-\alpha\left(v_1^2+v_2^2\right)-\frac{x_i}{l}\frac{v_1+v_2}{v_i}} \ldots \quad (23)
\end{aligned}$$

with $v_i = \|\vec{v}_1 - \vec{v}_2\|$. In passing we take a look at the distribution of $x_i$ in Fig. 5. The joint distribution (23) implies that $x_i$ is approximately distributed according to an exponential fall off, as one may expect, because the distances in the laboratory frame follow such a law. However there are differences: the mean is lower, e.g. $<x_i> \approx 0.71\,l$ for $D = 2$, and the distribution falls off faster than exponentially for small $x_i$ (cf. [23]).

## V. THE EXPANSION OF VELOCITY SPACE

We aim to compute the determinant of the matrix $M$ as defined by Eq. (13). There are always two distinct deviation matrices $M_{\mathrm{bound}}$ for $v_i < v_{\mathrm{crit}}$ and $M_{\mathrm{scatt}}$ for

$v_\mathrm{i} > v_\mathrm{crit}$, so that the phase space average naturally decomposes into

$$\langle \ln|\det M|\rangle = \langle \ln|\det M_\mathrm{bound}|\rangle_{v_\mathrm{i}<v_\mathrm{crit}}$$
$$+ \langle \ln|\det M_\mathrm{scatt}|\rangle_{v_\mathrm{i}>v_\mathrm{crit}} .$$

After determining these matrices, Eq. (10) will enable us to compute

$$\frac{h_\mathrm{KS}}{N} = \frac{\nu}{2} \left[ \; \langle \ln|\det M_\mathrm{bound}|\rangle_{v_\mathrm{i}<v_\mathrm{crit}} \right.$$
$$\left. + \langle \ln|\det M_\mathrm{scatt}|\rangle_{v_\mathrm{i}>v_\mathrm{crit}} \right] . \qquad (24)$$

Because of momentum conservation, $\vec{V}_\mathrm{i} = \vec{V}_\mathrm{f}$, the matrix $M$ is of the blocked form

$$M = \begin{pmatrix} \mathbb{1}_D & \Theta_D \\ \Theta_D & M' \end{pmatrix} ,$$

where $\mathbb{1}_D$ and $\Theta_D$ are unity and zero matrices of dimension $D \times D$ respectively. Therefore the only contribution to the growth in velocity space stems from the relative velocities,

$$\det M = \det M' . \qquad (25)$$

The final relative velocity [37] is

$$\vec{v}_\mathrm{f} = \sqrt{v_\mathrm{i}^2 - v_\mathrm{loss}^2} \left(\cos\vartheta \; \vec{e}_x + \sin\vartheta \; \vec{e}_y\right) . \qquad (26)$$

As defined in (16) $\vec{e}_x$ points in the direction of the incoming velocity and $\vec{e}_y = \vec{e}_x \times \frac{\vec{r}\times\vec{v}_\mathrm{i}}{\|\vec{r}\times\vec{v}_\mathrm{i}\|} = \frac{\vec{r}v_\mathrm{i}^2 - \vec{v}_\mathrm{i}\,(\vec{r},\vec{v}_\mathrm{i})}{\|\vec{r}v_\mathrm{i}^2 - \vec{v}_\mathrm{i}\,(\vec{r},\vec{v}_\mathrm{i})\|}$ is the orthogonal vector spanning the plan of motion, such that

$$\vec{r} = -X_\mathrm{i}\vec{e}_x + b\vec{e}_y$$

with $X_\mathrm{i} = x_\mathrm{i} + x_\mathrm{col}$ and $x_\mathrm{col} = -(\vec{r}_\mathrm{col},\vec{e}_x) = \sqrt{\sigma^2 - b^2}$ is the $x$-distance of the particles in the moment of collision.

When considering deviations of (26) one has to take into account contributions due to the change of the angle [38] $\vartheta = \vartheta(b(\vec{r},\vec{v}_\mathrm{i}),v)$,

$$\delta\vartheta = \frac{\partial\vartheta}{\partial b}\delta b + \frac{\partial\vartheta}{\partial b}\frac{X_\mathrm{i}}{v_\mathrm{i}}\delta v_y + \frac{\partial\vartheta}{\partial v_\mathrm{i}}\delta v_x , \qquad (27)$$

as well as contributions caused by rotations and inclinations of the orbital plane of motion:

$$\begin{pmatrix} \delta\vec{e}_x \\ \delta\vec{e}_y \\ \delta\vec{e}_z \\ \vdots \end{pmatrix} = \begin{pmatrix} 0 & \frac{\delta v_y}{v_\mathrm{i}} & \frac{\delta v_z}{v_\mathrm{i}} & \cdots \\ -\frac{\delta v_y}{v_\mathrm{i}} & 0 & \frac{X_\mathrm{i}}{b}\frac{\delta v_z}{v_\mathrm{i}} & \cdots \\ -\frac{\delta v_z}{v_\mathrm{i}} & -\frac{X_\mathrm{i}}{b}\frac{\delta v_z}{v_\mathrm{i}} & 0 & \\ \vdots & \vdots & & \ddots \end{pmatrix} \begin{pmatrix} \vec{e}_x \\ \vec{e}_y \\ \vec{e}_z \\ \vdots \end{pmatrix} . \qquad (28)$$

The Eqs. (27) and (28) hold for arbitrary spatial dimension $D$. The resulting deviation matrix $M'$ is rather complicated:

$$M' = \begin{pmatrix} \frac{\cos\vartheta}{\epsilon} - \epsilon v_\mathrm{i}\vartheta_v \sin\vartheta & -(1 + X_\mathrm{i}\vartheta_b)\,\epsilon\sin\vartheta & 0 & \cdots \\ \frac{\sin\vartheta}{\epsilon} + \epsilon v_\mathrm{i}\vartheta_v \cos\vartheta & +(1 + X_\mathrm{i}\vartheta_b)\,\epsilon\cos\vartheta & 0 & \cdots \\ 0 & 0 & \epsilon\left(\cos\vartheta + \frac{X_\mathrm{i}}{b}\sin\vartheta\right) & 0 & \cdots \\ & & 0 & \epsilon\left(\cos\vartheta + \frac{X_\mathrm{i}}{b}\sin\vartheta\right) & \\ \vdots & \vdots & \vdots & & \ddots \end{pmatrix} \qquad (29)$$

with the restitution coefficient (4) and the abbreviations $\vartheta_b \equiv \frac{\partial\vartheta}{\partial b}$, $\vartheta_v \equiv \frac{\partial\vartheta}{\partial v}$. The determinant of $M$ (which equals $M'$, cf. Eq. (25)) is surprisingly simple:

$$\det M = \left(-1 + x_\mathrm{i}\frac{\partial\vartheta}{\partial b}\right)\left(1 - \frac{v_\mathrm{loss}^2}{v_\mathrm{i}^2}\right)^{\frac{D}{2}-1}$$
$$\times \left(1 + \frac{x_\mathrm{i}}{b}\sin\vartheta\right)^{D-2} , \qquad (30)$$

where we eliminated $x_\mathrm{coll} \ll x_\mathrm{i}$ using

$$x_\mathrm{coll}\vartheta_b \approx -2$$
$$\frac{x_\mathrm{coll}}{b}\sin\vartheta \approx 2 - 2\frac{b^2}{\sigma^2}$$
$$\cos\vartheta \approx 2\frac{b^2}{\sigma^2} - 1 .$$

This reduces in the dry case, $v_\mathrm{loss} = 0$, to the expressions (18) ($D$=2) and (19) ($D$=3) in [23]. The first factor in (30) is always non-zero since $\frac{\partial\vartheta}{\partial b} < 0$.

## VI. RESULTS FOR THE KOLMOGOROV-SINAI ENTROPY

In Fig. 6 the relative dynamic $\vec{r}(t)$ (which equals the motion of one of the two particles in the center of mass system up to a factor of 2) is sketched. In both cases, the determinant of $M$ is of the form (30), but the meaning of the angle $\vartheta(b,v_\mathrm{i})$ is quite different. For impact velocities above the critical value, $\vartheta$ is the scattering angle

$$\vartheta_\mathrm{scatter}(b,v_\mathrm{i}) = \pi - \arcsin\frac{b}{\sigma}$$
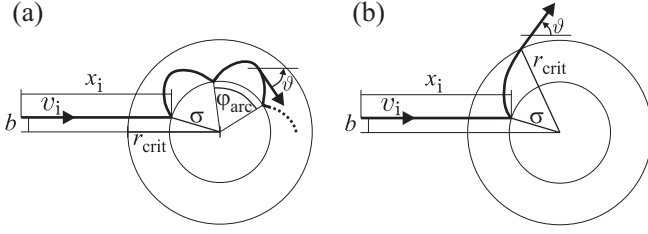
FIG. 6: The relative motion for (a) sticking and (b) scattering.

$$- \ \arcsin \frac{b}{r_{\text{crit}} \sqrt{1 - \left(\frac{v_{\text{loss}}}{v_{\text{i}}}\right)^2}}$$

$$- \ \int_\sigma^{r_{\text{crit}}} \mathrm{d}\varphi_\phi(r) \ ,$$

whereas for $v_{\text{i}} < v_{\text{critical}}$ the angle $\vartheta$ is a function of time,

$$\vartheta_{\text{bound}}(t_3, b, v_{\text{i}}) = \frac{\pi}{2} - \arcsin \frac{b}{\sigma}$$
$$- \ t_3 \frac{\varphi_{\text{arc}}(b, v_{\text{i}})}{t_{\text{arc}}(b, v_{\text{i}})} - \varphi_{\text{osc}}(t_3, b, v_{\text{i}}) \ .$$

Here $t_3$ denotes the time during which the two-particle systems remains bound until it is freed by a third particle. The angle between two contacts $\varphi_{\text{arc}}(b, v_{\text{i}})$ equals $2 \int_\sigma^{r_{\text{max}}(b, v_{\text{i}})} \mathrm{d}\varphi_\phi(r)$ and there is a similar integral for the time $t_{\text{arc}}$ it takes to run through one arc. The index $\phi$ ought to remind us that the potential (3) enters only through these integral expressions. For $t_3 \gg t_{\text{arc}}$ the angle $\vartheta_{\text{bound}}$ grows linearly with time, while the bound oscillations $\varphi_{\text{osc}}$ are negligible.

Depending on the details of the interaction potential, $\varphi_{\text{arc}}$ and $t_{\text{arc}}$ can grow beyond all bounds as the pair $(b, v_{\text{i}})$ approaches the critical line $(b, v_{\text{crit}}(b))$ (cf. Fig. 2) in the bound regime (from below). This singular behavior occurs in the Extended Capillary Model (linear force, Fig. 1), whereas in the Minimal Capillary Model (constant force) both quantities remain finite. Close to the divergence the motion is an outward directed spiral, so that the turning point is never reached and the periodic collisions end. The interaction time can also diverge for scattering states (reaching the critical line in Fig. 2 from top), but this singularity is integrable with respect to velocity. In the bound case the divergence is cut off by the third particle and because of angular momentum conservation we have the estimate

$$\vartheta_{\text{bound}}(t_3, b, v_{\text{i}}) \leq \text{const} + \frac{t_3 b v_{\text{i}}}{\sigma^2} \ . \tag{31}$$

We will use the right-hand side as an approximation. The stopping time $t_3$ is a random variable itself and distributed according to

$$\frac{V_{\text{i}}}{l'} \ \mathrm{e}^{-\frac{V_{\text{i}}}{l'} t_3} \ \mathrm{d}t_3 \ , \tag{32}$$

for a given center of mass velocity $V_{\text{i}}$ of the bound system. There is a smaller mean free path $l'$ for the bound two-particle system: since its total cross section changes with time the effective diameter $\sigma_{\text{eff}}$ is $\frac{3}{2}\sigma$ so that the mean center-center distance at contact is $\frac{5}{4}\sigma$. Another factor of $\sqrt{\frac{2}{3}}$ is caused by the mass ratio [31], thus

$$l' = \left(\frac{4}{5}\right)^{D-1} \sqrt{\frac{2}{3}} l \ . \tag{33}$$

In the following, we shall evaluate averages that are linear in $t_3$, so that we can forthwith substitute the expectation value, $\overline{t_3} = \frac{l'}{V_{\text{i}}}$, of the distribution (32). Then from (31) follows

$$\frac{\partial \vartheta_{\text{bound}}}{\partial b}(v_{\text{i}}) \approx \frac{v_{\text{i}} \ l'}{V_{\text{i}} \ \sigma^2} \ . \tag{34}$$

In both cases, binding and scattering, $\frac{\partial \vartheta}{\partial b}$ is at least of the order of $\frac{1}{\sigma}$, while $x_{\text{i}}$ is of the order of the mean free path

$$l = \frac{\Gamma\left(\frac{D+1}{2}\right)}{\sqrt{2}\pi^{\frac{D-1}{2}}} \left(\sigma^{D-1} n\right)^{-1} \ , \tag{35}$$

with $n$ being the number density of grains. Formulas for the mean free path are well established [30] and other characteristic quantities for the motion of tracer particles are also available [31]. We remark that investigating the trajectories of tracer particles is a promising technique for the experimental confirmation of results presented in this article.

Our goal is to expand the KSE in the small dimensionless parameter $n\sigma^D \ll 1$. So this is an expansion for the dilute wet granular system. The unity in the first and the last factor in (30) contributes to the KSE only in linear and higher orders, while we are interested in the logarithmic and zeroth order terms:

$$|\det M| = x_{\text{i}} \left|\frac{\partial \vartheta}{\partial b}\right| \left(1 - \frac{v_{\text{loss}}^2}{v_{\text{i}}^2}\theta(v_{\text{i}} - v_{\text{crit}})\right)^{\frac{D}{2}-1}$$
$$\times \left(\frac{x_{\text{i}}}{b}\sin\vartheta\right)^{D-2} \ . \tag{36}$$

With the step function $\theta$, Eq. (36) is valid for scattering and binding, because we assume that the collision with the third particle rethermalize the two-particle system, so that the next collision cycle starts with the same initial distribution. Since the 'third' particles have an energy of the order of the granular temperature $T \gg E_{\text{loss}}$ we can safely neglect the formation of bound states of three or more particles (cf. Fig. 10). A cluster size expansion will be discussed at the end of this section.

After introducing the appropriate length scales $l$ and $\sigma$ we are lead to examine

$$\frac{h_{\text{KS}}}{N} = \frac{\nu}{2}\left[(D-1)\ln\frac{l}{\sigma} - (D-2)\left\langle\ln\frac{b}{\sigma}\right\rangle\right.$$

$$+ (D-1)\left\langle \ln \frac{x_\mathrm{i}}{l} \right\rangle$$

$$+ \left\langle \ln\left( \sigma \left| \frac{\partial \vartheta_\mathrm{bound}}{\partial b} \right| \right) \right\rangle_{v_\mathrm{i} < v_\mathrm{crit}}$$

$$+ \left\langle \left(\frac{D}{2}-1\right) \ln \epsilon + \ln\left( \sigma \left| \frac{\partial \vartheta_\mathrm{scatt}}{\partial b} \right| \right) \right\rangle_{v_\mathrm{i} > v_\mathrm{crit}}$$

$$+ (D-2)\left\langle \ln|\sin\vartheta| \right\rangle \Bigg] . \tag{37}$$

The first two terms in the square bracket yield

$$- \ln n\sigma^D - C_D \ , \tag{38}$$

with a numerical constant $C_D = \frac{D-1}{2}\ln 2 + \frac{(D-1)^2}{2}\ln\pi - \frac{D-2}{D-1} - (D-1)\ln\Gamma\left(\frac{D+1}{2}\right)$. This is independent of the ensemble average and the interaction potential.

If $x_\mathrm{i}$ was distributed exponentially with mean $l$, the third term in (37) would give rise to the negative of Euler's constant, $-\gamma_\mathrm{Euler} \approx -0.5772$, independent of the dimensionality of the problem. As discussed before, lower values of $x_\mathrm{i}$ are favored. That is why we find by numerical computation a lower expectation value, e.g. for $D=2$:

$$\left\langle \ln \frac{x_\mathrm{i}}{l} \right\rangle \approx -1.01. \tag{39}$$

The fourth term in (37) is (cf. Eq. (34))

$$\left\langle \ln\left( \sigma \left| \frac{\partial \vartheta_\mathrm{bound}}{\partial b} \right| \right) \right\rangle_{v_\mathrm{i} < v_\mathrm{crit}}$$

$$= -\left( \ln n\sigma^D + \tilde{C}_D \right)\langle 1 \rangle_{v_\mathrm{i} < v_\mathrm{crit}}$$

$$+ \left\langle \ln \frac{v_\mathrm{i}}{V_\mathrm{i}} \right\rangle_{v_\mathrm{i} < v_\mathrm{crit}} , \tag{40}$$

with the numerical constant $\tilde{C}_D = (D-1)\ln\frac{5}{4} + \frac{\ln 3}{2} + \frac{D-1}{2}\ln\pi - \ln\Gamma\left(\frac{D+1}{2}\right)$.

Together with (38) the logarithm $\ln n\sigma^D$ herein forms the leading term of the density expansion. Therefore the logarithm $\ln n\sigma^D$ in (40) is a correction of the leading term as it is known for the dry case [23]. The KSE has the following density expansion:

$$\frac{h_\mathrm{KS}}{N} = -\nu A_D \ln n\sigma^D + \nu B_D + \mathcal{O}(n\sigma^D), \tag{41}$$

with the leading coefficient

$$A_D = A_D\left( \frac{E_\mathrm{loss}}{T}, \frac{r_\mathrm{crit}}{\sigma} \right)$$

$$= \frac{D-1}{2} + \frac{D-1}{\Gamma(\frac{D}{2})}\left(\frac{m}{4T}\right)^{\frac{D}{2}}$$

$$\times \int_0^\sigma \frac{\mathrm{d}b\, b^{D-2}}{\sigma^{D-1}} \int_0^{v_\mathrm{crit}(b)} \mathrm{d}v\, v^{D-1}\, \mathrm{e}^{-\frac{m}{4T}v^2} , \tag{42}$$

and the density independent part

$$B_D = \frac{1}{2}\Big[ -C_D + (D-1)\left\langle \ln \frac{x_\mathrm{i}}{l} \right\rangle - \tilde{C}_D\langle 1 \rangle_{v_\mathrm{i} < v_\mathrm{crit}}$$

$$+ \left\langle \ln \frac{v_\mathrm{i}}{V_\mathrm{i}} \right\rangle_{v_\mathrm{i} < v_\mathrm{crit}} + \left\langle \ln\left( \sigma \left| \frac{\partial \vartheta_\mathrm{scatt}}{\partial b} \right| \right) \right\rangle_{v_\mathrm{i} > v_\mathrm{crit}}$$

$$+ (D-2)\left( \frac{\langle \ln \epsilon \rangle_{v_\mathrm{i} > v_\mathrm{crit}}}{2} + \langle \ln|\sin\vartheta| \rangle \right) \Big]. \tag{43}$$
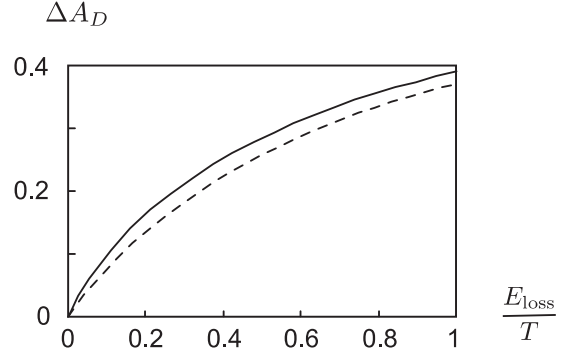


FIG. 7: The increase $\Delta A_D = \frac{P_\mathrm{bound}}{2}$ of the leading coefficient $A_D = \frac{D-1}{2} + \Delta A_D$: The solid line is for two, the dashed line for three dimensions $D$. Since $A = \frac{D-1}{2}$ in the absence of the liquid bridge interaction we recover the result for dry granulates as a special case. With the approximation for the wet granular gas used in the derivations one is restricted to temperatures above the bridge energy $E_\mathrm{loss}$. Otherwise the method applied has to be extended to take clusters of more than two particles sticking together into account. The far extreme case, $E_\mathrm{loss} \gg T$, is known as the so-called sticky gas.

The general form of the leading term, valid for any velocity distribution, is

$$A_D = \frac{D-1}{2} + \frac{P_\mathrm{bound}}{2} . \tag{44}$$

We want to emphasize that so far all results of this section are general with respect to the spatial dimensionality of the problem and the details of the particle interaction. The probability $P_\mathrm{bound} = \langle 1 \rangle_{v_\mathrm{i} < v_\mathrm{crit}}$ in (44) is given by integrating velocity and impact factor over the bound states in Fig. 2. Only here the detailed interaction models (6) and (7) enter the problem.

Let us now turn to explicit results. For the Gaussian velocity distribution (15) and odd spatial dimensions the velocity integral of $P_\mathrm{bound}$ is an incomplete Gamma function. In even dimensions the integral is elementary, yielding for $D=2$

$$A_2(\varepsilon, \gamma) = 1 - \frac{1}{2}\int_0^1 \mathrm{d}x\, \mathrm{e}^{-\varepsilon\, f(x,\gamma)}, \quad \varepsilon = \frac{E_\mathrm{loss}}{T},$$

as a function of the bridge energy over granular temperature, $\varepsilon$, and the wetting content, $\gamma = r_\mathrm{crit}/\sigma \geq 1$. The remaining integration variable is the impact parameter, $x = b/\sigma$. The excess of the critical energy over the bridge energy, $f(x,\gamma) = E_\mathrm{crit}/E_\mathrm{loss}$, depends on the model details. In the Minimal Capillary Model from Eq. (7) follows

$$f(x,\gamma) = \left( 1 - \frac{x^2}{\gamma^2} \right)^{-1} .$$

The coefficient $A_D$ of the Minimal Capillary Model is plotted in Fig. 7 as a function of the liquid bridge energy

for two and three dimensions. Very similar curves follow from the Extended Capillary Model. For the plot the limit of short liquid bridges, $r_{crit} = \sigma$, was chosen. This corresponds to a small amount of liquid that is just sufficient to wet the surface roughness of realistic spheres. Independent of $r_{crit}/\sigma \geq 1$, in the dry limit (or equivalently the high temperature limit) $A_D$ approaches $(D-1)/2$, which is the known result for hard spheres [23]. For a higher content of wetting liquid, $r_{crit}/\sigma > 1$, the dependence of the leading term on the binding energy becomes flatter, but in an experimental situation there is a simultaneous gain in $E_{loss}$ when liquid is added. Varying the surface tension of water by adding a salt to the wetting solution is an experimentally feasible way to measure this curve directly with a fixed amount of wetting liquid, such that $r_{crit}/\sigma$ can be kept constant.

From this graph we see the sensitive dependence of the KSE on the cohesion force of the wetting liquid. To gain analytic insight we investigate exemplarily the two-dimensional case plotted. Substituting $z = 1/(1 - x^2)$ gives

$$A_2(\varepsilon, 1) = 1 - \frac{1}{4} \int_1^\infty \frac{dz}{z^2} \frac{e^{-\varepsilon z}}{\sqrt{1 - 1/z}} \qquad (45)$$

Splitting up the integration at $z = 1/\varepsilon$ allows to separate the non-analytic part.

$$A_2(\varepsilon, 1) = 1 - \frac{\varepsilon}{4} \int_1^\infty \frac{dz}{z^2} \frac{e^{-z}}{\sqrt{1 - \varepsilon/z}}$$
$$- \frac{1}{4} \int_1^{\frac{1}{\varepsilon}} \frac{dz}{z^2} \frac{e^{-\varepsilon z}}{\sqrt{1 - 1/z}} \qquad (46)$$

The first integral in (46) can be expanded in powers of $\varepsilon \in [0, 1)$ since $z > 1$. The second integral equals 2 for $\varepsilon \to 0$, while its first derivative has a logarithmic divergence:

$$A_2(\varepsilon, 1) = \frac{1}{2} + \varepsilon \left( C - \frac{\ln \varepsilon}{4} \right) + \mathcal{O}(\varepsilon^2) . \qquad (47)$$

The constant $C$ is $\int_1^\infty \exp(-z)/4z + \ln 2/2 + (1 - 1/e)/4 \approx 0.56$. This shows that the slope of $A_2$ is vertical at $E_{loss} = 0$.

Let us finally look at the next higher order term $B_D$ of the density expansion. For simplicity we restrict ourselves to the case $D = 2$, so that

$$B_2 = \frac{1}{2} \left[ -C_2 + \left\langle \ln \frac{x_i}{l} \right\rangle - \tilde{C}_2 \left\langle 1 \right\rangle_{v_i < v_{crit}} + \left\langle \ln \frac{v_i}{V_i} \right\rangle_{v_i < v_{crit}} \right.$$
$$\left. + \left\langle \ln \left( \sigma \left| \frac{\partial \vartheta_{scatt}}{\partial b} \right| \right) \right\rangle_{v_i > v_{crit}} \right]. \qquad (48)$$

The last term in (48) is exactly equal to unity in the limit of dry granulates,

$$\lim_{E_{loss} \to 0} \left\langle \ln \left( \sigma \left| \frac{\partial \vartheta_{scatt}}{\partial b} \right| \right) \right\rangle_{v_i > v_{crit}}$$
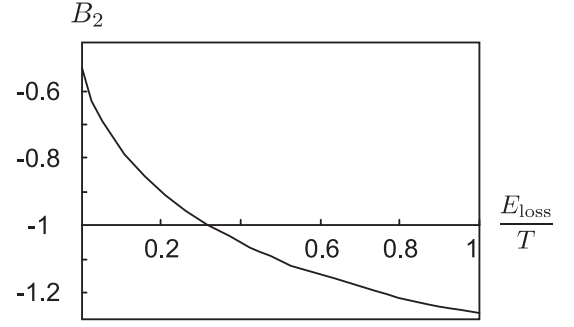


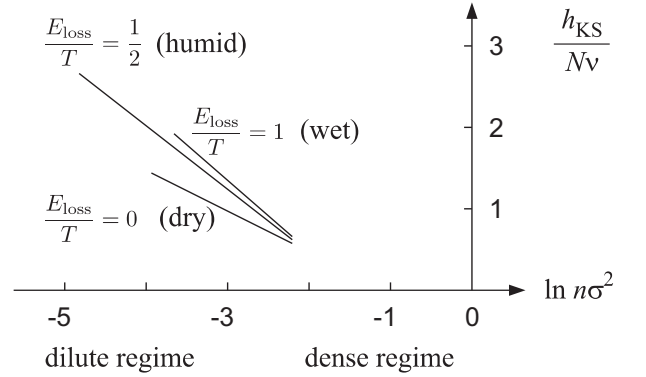FIG. 8: The coefficient $B_2$ of the density expansion (41).



FIG. 9: The two-dimensional KSE as a function of the density for three different bridge energies $E_{loss}$. This energy depends on the amount of wetting liquid added to the granular gas as is indicated in the plot. Another way to change $E_{loss}$ is to add a salt or a surfactant.

$$= \int_0^\sigma \frac{db}{\sigma} \ln \frac{2}{\sqrt{1 - \left( \frac{b}{\sigma} \right)^2}} = 1 ,$$

but decreases as the critical velocity increases when we turn on the liquid bridge interaction. The coefficient $B_2$ for the zeroth order in the expansion (41) is plotted in Fig. 8. It is known for the dry limit [23], that the accordance of $B_D$ with numerical simulation cannot keep up with the successful confirmation of $A_D$. The origin of this discrepancy is the assumption that the unstable manifold coincides with velocity space and it is quite involved to improve on that [32]. In the dry limit our method yields $B_2 = -0.52(8)$, which is lower than the analytical estimate ($B_2 = 0.1045$) and the simulated result ($B_2 = 0.679$) of [23].

From the knowledge of the coefficients $A_D$ and $B_D$ follows the KSE in the dilute system for various wetting contents as shown in Fig. 9 for $D = 2$.
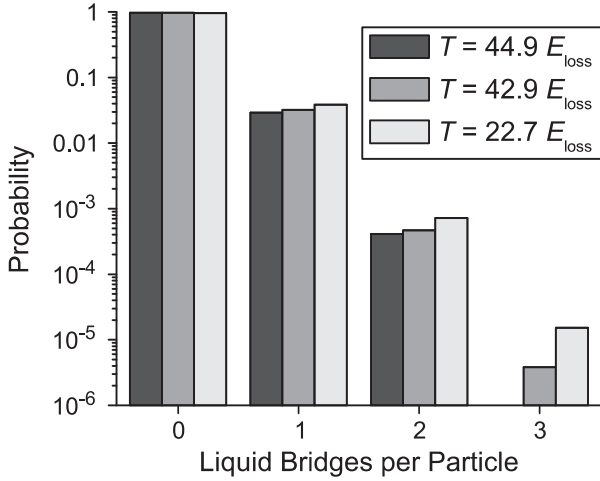
FIG. 10: The probability for a sphere to have a certain number of liquid bonds ending on its surface. This distribution is measured in a three dimensional molecular dynamics simulation of a wet granular gas with an occupied volume fraction of 3.9%, which corresponds to $n\sigma^3 = 0.074$. The granular temperature $T$ has been varied as indicated. The probability for two liquid bridges ending on one particle, as necessary for a three-particle-cluster, is suppressed by more than three orders of magnitude. An analytic approach to the KSE is favorable because the direct numerical integration suffers from high computing times for the full tangent space dynamics and yields noisy results [33, 35]. The liquid bond distribution shown is a robust and reliable single-particle quantity.

### The Cluster Expansion

In Eq. (24) we considered events including bound states of two particles $(a + b + c \rightarrow ab + c \rightarrow a + b + c)$ and scattering events $(a + b \rightarrow a + b)$ by writing

$$
\begin{aligned}
\langle \ln | \det M | \rangle &= \langle \ln | \det M_{\text{bound}} | \rangle_{v_i < v_{\text{crit}}} \\
&+ \langle \ln | \det M_{\text{scatt}} | \rangle_{v_i > v_{\text{crit}}} \; .
\end{aligned} \quad (49)
$$

The first term is proportional to $P_{\text{bound}}$ which led to Eq. (44). Here we wish to point out how to generalize the computation of the KSE to include clusters of higher particle number. All equalities in (10) hold for arbitrary types of events, when $M_i$ denotes the deviation matrix associated with the $i$th event and $\nu$ is the generalized event frequency. Referring to the event type by T we reorder the averaging. Collecting the events of type T by introducing $\delta_{\text{type}(j),\text{T}}$ (which is unity for an event T and otherwise zero) we write $\langle \ldots \rangle_{\text{T}}$ for $\langle \ldots \delta_{\text{type}(j),\text{T}} \rangle$:

$$
\frac{2}{\nu N} h_{\text{KS}} = \langle \ln | \det M | \rangle = \sum_{\text{T}} \langle \ln | \det M_{\text{T}} | \rangle_{\text{T}} \; . \quad (50)
$$

The summation can be written as a systematic expansion in the cluster size:

$$
\begin{cases}
a + b \rightarrow a + b & (\text{T}_1) \\
\qquad\qquad\qquad a + b + c & (\text{T}_2) \\
\qquad\qquad \nearrow \\
a + b + c \rightarrow ab + c \;\; \rightarrow \begin{cases} ac + b & (\text{T}_3) \\ bc + a & (\text{T}_4) \\ ab + c & (\text{T}_5) \end{cases} \\
\qquad\qquad \searrow \\
\qquad\qquad\qquad abc & (\text{T}_6) \\
\vdots
\end{cases}
$$

with the events $\text{T}_1$ and $\text{T}_2$ considered before in (49). The events $\text{T}_j$ with $j > 2$ result in new many-particle-clusters which are exponentially rare components of the wet granular gas as is evident from Fig. 10. We remark that the scattering of a bound state ($\text{T}_5$) prolongs the mean bond time $t_3$ to become $t_3' = \alpha t_3$, with $\alpha = 1 + 2P_{\text{T}_5} + 3P_{\text{T}_5}^2 + \ldots = 1/(1 - P_{\text{T}_5})^2$. The unity in front of this series corresponds to breaking the bound state in its first collision ($\text{T}_2$), the second term corresponds to one scattering event of the bound pair and the following terms to multiscattering. The contribution to the KSE is proportional to the logarithm of this time, $\ln t_3' = \ln t_3 - 2 \ln(1 - P_{\text{T}_5})$. The first term $\ln t_3 \propto -\ln(n\sigma^D)$ is the wet granular contribution to the leading coefficient $A$ as identified in Eq. (44). The second term gives a correction to the $B$-coefficient which is of the order $P_{\text{T}_5} = \mathcal{O}\left(\sqrt{E_{\text{loss}}/T}^3\right)$ for three dimensions.

## VII.   CONCLUSIONS

### Summary

We worked out the crucial difference in the interaction of wet granulates compared to the dry case. There is a liquid bridge causing a radial hysteretic force over finite distance. The detailed distance dependence is of minor importance. The decisive ingredient in the Capillary Model is the extraction of a bridge energy that is independent of the initial velocity in contrast to the "Standard Model" using a restitution to extract a certain fraction of energy.

We found an enhanced chaotic behavior of the wet granular system. The leading term in the expansion of the KSE with respect to the small density $(n\sigma^2 \ll 1)$ changed due to the possible sticking of particles. One can think of the prolonged interaction time enforcing the exponential separation in velocity space. The continuous but in general not differentiable transition to the limiting dry case has been established.

This dynamical property recommends the wet granular system as a suitable candidate for experimental, numerical and analytic tests of the Gallavotti-Cohen fluctuation theorem [34] which requires hard chaos.

## Outlook

In this analytic work we used an assumption on the unstable manifold and we neglected correlation effects in consecutive collisions. Although physically motivated, the next challenge will be to verify these assumptions by direct numerical simulations.

The rigorous derivation of phenomenological laws such as the Navier-Stokes equation for viscous flow and the Fourier law for heat transport is a fundamental problem under intense discussion. Relations between the Lyapunov spectrum of the microscopic dynamics and macroscopic properties such as viscosity and heat conductivity have been established within the last years, most detailed for the Lorentz gas [16, 17, 18, 19, 20, 21, 22]. The severity and importance of these relations become apparent from the fact they have to bridge the gap between microscopic reversibility and macroscopic irreversibility challenging physicists since Ludwig Boltzmann.

The dynamics of the wet granular system studied in this work follows a mesoscopic law including dissipation, and kinetic theory has already been extended to dry granular matter [2]. The next step is to extend also these transport relations. We hope that our results on the Lyapunov exponents might stimulate this development. On the experimental side mechanical properties of wet granulates are presently under investigation [7].

A further interesting problem is the computation of the KSE for dense wet granulates. This might lead to a novel description of clustering – as a non-equilibrium phase transition – in terms of the Lyapunov spectrum. Yet this problem is challenging as it needs new concepts, because the identification of the velocity space with the instable manifold is limited to the dilute gas.

## Acknowledgments

[1] I. Goldhirsch, Ann. Rev. Fluid Mech. **35**, 267 (2003).

[2] N. V. Brilliantov and T. Pöschel, *Kinetic Theory of Granular Gases* (Oxford University Press, 2004).

[3] J. W. Dufty and J. J. Brey, J. Stat. Phys. **109**, 433 (2002).

[4] A. Zippelius, Physica A **369**, 143 (2006).

[5] S. Herminghaus, Adv. Phys. **54**, 221 (2005).

[6] M. Schulz, B. M. Schulz, and S. Herminghaus, Phys. Rev. E **67**, 052301 (2003).

[7] Z. Fournier *et al.*, J. Phys.: Condens. Matter **17**, S477 (2005).

[8] S. Taibi, A. Alem, and J. M. Fleureau, *Powders and Grains*, 605 (Taylor & Francis, 2005);
M. Lenoble, *et al.*, *loc. cit.*, 621;
O. Pozo, N. Fraysse, and N. Olivi-Tran, *loc. cit.*, 625.

[9] J. Y. Delenne, M. S. El Youssoufi, F. Cherblanc, and J. C. Benet, Int. J. Num. Anal. Meth. Geom. **28**, 1577 (2004);
V. Richefeu, M. S. El Youssoufi, and F. Radjaï, Phys. Rev. E **73**, 051304 (2006).

[10] V. Yu. Zaburdaev, M. Brinkmann, and S. Herminghaus Phys. Rev. Lett. **97**, 018001 (2006).

[11] A. Fingerle and S. Herminghaus, Phys. Rev. Lett. **97**, 078001 (2006).

[12] A. Fingerle, S. Herminghaus, and V. Zaburdaev, Phys. Rev. Lett. **95**, 198001 (2005).

[13] H. Kantz and T. Schreiber, *Nonlinear Time Series Analysis* (Cambridge University Press, 1997).

[14] Ya. B. Pesin, Usp. Mat. Nauk. **32** No. 4, 55 (1977)
[ Russian Math. Surveys **32**(4), 55 (1977) ].

[15] J.-P. Eckmann and D. Ruelle, Rev. Mod. Phys. **57**, 617 (1985).

[16] P. Gaspard, Phys. Lett. A **168**, 13 (1992).

[17] P. Gaspard and G. Nicolis, Phys. Rev. Lett. **65**, 1693 (1990).

[18] J. R. Dorfman and P. Gaspard, Phys. Rev. E **51**, 28 (1995).

[19] A. Baranyai, D. J. Evans, and E. G. D. Cohen, J. Stat. Phys. **70**, 2209 (1993).

[20] N. I. Chernov, G. L. Eyink, J. L. Lebowitz, and Ya. G. Sinai, Phys. Rev. Lett. **70**, 2209 (1993).

[21] N. I. Chernov, G. L. Eyink, J. L. Lebowitz, and Ya. G. Sinai, Commun. Math. Phys. **154**, 569 (1993).

[22] S. Viscardy and P. Gaspard, Phys. Rev. E **68**, 041205 (2003).

[23] H. van Beijeren, J. R. Dorfman, H. A. Posch, and Ch. Dellago, Phys. Rev. E **56**, 5272 (1997).

[24] J. R. Dorfman, A. Latz, and H. van Beijeren, Chaos **8**, 444 (1998).

[25] S. J. R. Simons, J. P. K. Seville, and M. J. Adams, Chem. Eng. Sci. **49**, 2331 (1994).

[26] Ch. D. Willett, M. J. Adams, S. A. Johnson, and J. P. K. Seville, Langmuir **16**, 9396 (2000).

[27] V. I. Oseledec, Trudy Mosk. Mat. Obsch. **19**, 179-210 (1968)
[ Trans.: Moscow Math. Soc. **19**, 197 (1968) ].

[28] N. Simanyi, Ergod. Theo. Dyn. Sys. **19**, 741 (1999).

[29] O. Herbst, P. Müller, M. Otto, and A. Zippelius, Phys. Rev. E **70**, 051313 (2004).

[30] N. Chernov, Vienna, Preprint ESI 410 (1996).

[31] P. Gaspard and H. van Beijeren, J. Stat. Phys. **109**, 671 (2002).

[32] A. S. de Wijn, Phys. Rev. E **71**, 046211 (2005).

[33] H. L. Yang and G. Radons, Phys. Rev. E **71**, 036211 (2005).

[34] G. Gallavotti and E. G. D. Cohen, Phys. Rev. Lett. **74**, 2694 (1995);
G. Gallavotti and E. G. D. Cohen, J. Stat. Phys. **80**, 931 (1995).

[35] The direct integration algorithm has to adapt the time steps to allow for an accurate integration of the extremely short contact repulsion. With these fine integration steps

it takes extremely long until the system has explored its high dimensional phase space as necessary for reliable Lyapunov spectra. Associated with the high number of integration steps is an increase of the numerical error. We remark that the superior event-driven technique is not applicable for the Capillary Model of wet granular matter in $D \geq 2$ dimensions.

[36] In the capillary regime described in [5], the dissipation by inelastic collisions [2] is dominated by the hysteretic liquid bridge interaction.

[37] Note that in this context $v_{\mathrm{loss}}$ is given by $mv_{\mathrm{loss}}^2/4 = \phi + E_{\mathrm{loss}}$ as a function of $r$ for the case of sticking particles, when 'final' does not refer to the rupture event.

[38] One has to distinguish between the variation of the function $b$ (as given in item (i) on page 5), $\delta b(\vec{r}_{\mathrm{i}}, \vec{v}_{\mathrm{i}}) = \delta(\vec{r}_{\mathrm{i}}, \vec{e}_y) = \delta b - \frac{X_{\mathrm{i}}}{v_{\mathrm{i}}}\delta v_y$, and $\delta b = (\delta\vec{r}_{\mathrm{i}}, \vec{e}_y)$ as an opportune notation for the spatial deviation $\delta y$.